

**Highlight Review**

# A Revisit to Molecular Orbitals in $\text{H}_2^+$ , LiH, HF, and Hybridization

Shin-ichi Nagaoka,\* Hiroyuki Teramae, and Umpei Nagashima

(Received November 17, 2011; CL-111113)

**Abstract**

We have drawn three-dimensional contour plots of  $\text{H}_2^+$  molecular orbitals and carbon hybrid orbitals according to explanations given in quantum chemistry textbooks and have also performed ab initio molecular orbital calculations of LiH and HF. Some contour representations and molecular orbital energy-level diagrams thus obtained are not consistent with the figures adopted in the textbooks. It is considered that the usual explanations for the molecular orbitals of  $\text{H}_2^+$ , LiH, HF, and hybridization in the conventional textbooks are liable to misunderstanding.

necessarily self-evident for most experimental chemists and university students. The inconsistency should be clearly pointed out somewhere.

Therefore, in the present paper, we revisit the MOs in  $\text{H}_2^+$ , LiH, HF, and hybridization. Ideas developed in treating these simple subjects also provide a basis for dealing with complex systems. Furthermore, the quantum chemistry of  $\text{H}_2^+$  and LiH is still a topic of current interest,<sup>7,8</sup> and it is needless to say that HF and hybridization play very important roles in chemistry.<sup>9a,9b,10</sup> Thus, our revisit to the MOs in  $\text{H}_2^+$ , LiH, HF, and hybridization in this review should shed new light on understanding of quantum chemistry.

**◆ Introduction**

The molecular orbital (MO) model is a most convincing method predicting molecular structures and functions. At the present time, even experimental chemists use MO theory for their own applications, and the method is also widely learned in university courses.<sup>1,2</sup> There, drawing orbital contour plots and energy level diagrams has a large impact on understanding of MO theory. The drawing helps us to grasp qualitative aspects of MO concepts pictorially. Because of explosive developments in computer hardware and software, orbital drawing and its widespread applications have become ordinary now.

Accordingly, in our university course, we make the students receive practical training of drawing MO contour plots by using Microsoft Excel,<sup>3,4</sup> which is useful in practical training of quantum chemistry.<sup>5,6</sup> Our practice helps the students to grasp the essential physical concepts of the MOs under various restraints such as time. However, during practice, we have found that some of the contour representations and MO energy-level diagrams obtained for hydrogen molecule ion ( $\text{H}_2^+$ ), lithium hydride (LiH), hydrogen fluoride (HF), and hybridization are not consistent with the figures adopted in the most recent editions of various textbooks of chemistry. It is thought that the usual explanations for their MOs are apt to be misleading.

We suppose that the authors of the textbooks know the limitation of their explanation, and to condense the textbooks they might have abbreviated description on the above-mentioned inconsistency self-evident for them. However, the matter self-evident for the authors and some theoretical chemists is not

**◆ Computational Method and Procedure**

The computational method and procedure have been described in previous papers.<sup>3,11</sup> Briefly, three-dimensional (3D) contour plots of  $\text{H}_2^+$  MOs and carbon hybrid orbitals were drawn with Microsoft Excel 2010. Although the  $\text{H}_2^+$  MOs are often drawn without normalization,<sup>6</sup> we here show the normalized MOs. The diatomic overlap integrals are then neglected. The effective nuclear charge  $3.25e^{12}$  was used in the drawing of the carbon hybrid orbitals. The orbital energies of LiH,  $\text{LiH}^+$ , HF, Li,  $\text{Li}^+$ , H,  $\text{H}^+$ ,  $\text{H}^-$ , F, and  $\text{F}^-$  were calculated at the level of HF/6-311++G\*\*<sup>13,14</sup> by using the Gaussian 03 program.<sup>15</sup> The restricted Hartree–Fock (RHF) and unrestricted Hartree–Fock (UHF) methods were employed for the closed- and open-shell species, respectively. To facilitate comparison,  $3\sigma_u$  MO of  $\text{H}_2^+$  ( $\text{H}_2^+:3\sigma_u$ ) was calculated at the level of UHF/6-31G(p) and visualized by using the GaussView program.

As mentioned in Introduction, the inconsistency with the figures adopted in some textbooks of chemistry has been found during practical training in our university course.<sup>3,4</sup> Reference 16 is used as the textbook. During practice, students draw the 3D contour plots of the  $\text{H}_2^+$  MOs and carbon hybrid orbitals and also plot out LiH MOs to learn the effect of ionic character. In addition, the practical training contains drawing graphs of radial functions and their distribution functions for hydrogen-like atoms to learn penetration in many-electron atoms.<sup>3,4</sup> Furthermore, the practice trainees learn a particle in a box, a harmonic oscillator, and Hückel approximation by using Microsoft Excel. Our graduate students also receive practical training of ab initio calculations<sup>2</sup> and of drawing the  $\text{H}_2^+$  MOs

Prof. Shin-ichi Nagaoka,\*<sup>1</sup> Prof. Hiroyuki Teramae,<sup>2</sup> and Dr. Umpei Nagashima<sup>3</sup>

<sup>1</sup>Department of Chemistry, Faculty of Science and Graduate School of Science and Engineering, Ehime University, Matsuyama, Ehime 790-8577

<sup>2</sup>Faculty of Science, Josai University, 1-1 Keyakidai, Sakado, Saitama 350-0295

<sup>3</sup>Nanosystem Research Institute, National Institute of Advanced Industrial Science and Technology, 1-1-1 Umezono, Tsukuba, Ibaraki 305-8568

E-mail: nagaoka@ehime-u.ac.jp

including polarization functions.<sup>4</sup> These exercises have a large educational impact on understanding of MO methods.

### ◆ Hydrogen Molecule Ion ( $H_2^+$ )

Hydrogen molecule ion  $H_2^+$  consists of two protons and one electron and furnishes many ideas useful for discussing many-electron molecules. As explained in various quantum chemistry textbooks, MOs of  $H_2^+$  can be described according to atomic orbitals (AOs) of the two hydrogen atoms obtained on dissociation (separated atom description<sup>1a</sup>). Then, to form a MO of  $H_2^+$ , an AO of one of the two H atoms linearly combines with the same AO of another H. In a simple quantum-chemical picture, the AO is given as the product of a radial function and a spherical harmonics function.<sup>1b,5,16a</sup> The 3D contour representations of  $1\sigma_g$  and  $1\sigma_u$  MOs ( $H_2^+:1\sigma_g$  and  $H_2^+:1\sigma_u$ , respectively) thus constructed are consistent with the figures adopted in various textbooks of quantum chemistry.<sup>3</sup>

On the other hand, Figure 1a shows the 3D contour representation of  $3\sigma_u$  MO ( $H_2^+:3\sigma_u$ ) similarly constructed.<sup>3</sup> This representation shows the orbital amplitude ( $\psi(3\sigma_u)$ ) in a plane containing the two H nuclei. The  $H_2^+:3\sigma_u$  MO is an antibonding orbital composed of two 2p AOs of hydrogen (H:2p's) that overlap head-to-tail along a line connecting the two H nuclei. The internuclear distance used in the plot was 2.00 au, which is the same as the stable internuclear distance of  $H_2^+$  in the ground state ( $X^2\Sigma_g^+$  state<sup>17</sup>).<sup>18</sup> The nuclear charge used was  $e$ . The MO shape shown in Figure 1a is similar to that of 2p AO. However, it should be noted that Figure 1a does not show the united-atom state<sup>1a</sup> for  $3\sigma_u$  because the united-atom state for  $3\sigma_u$  is not 2p but 4p as shown in Reference 1c.

In contrast to the cases of  $H_2^+:1\sigma_g$  and  $H_2^+:1\sigma_u$ , the contour plot of  $H_2^+:3\sigma_u$  shown in Figure 1a is not consistent with the figures adopted in various quantum chemistry texts.<sup>1d,19a</sup> In the textbooks, the  $H_2^+:3\sigma_u$  MO is drawn like Figure 2, which was obtained by our calculation using the ab initio MO method and thus shows the real picture of  $3\sigma_u$ . In Figure 2, positive- and negative-valued lobes (4 lobes in total) are aligned alternately along a line connecting the two H nuclei. However, in Figure 1a, two centered lobes are too small to be seen, and at first glance the  $H_2^+:3\sigma_u$  MO seems to be composed of only two lobes at both ends. Thus, the usual explanation that the  $H_2^+:3\sigma_u$  orbital is constructed as mentioned above may lead to confusion because of the inconsistency between Figures 1a and 2.

The above-mentioned inconsistency is avoided in the following computational results. Figure 1b shows the 3D contour representation of the  $H_2^+:3\sigma_u$  MO for the internuclear distance of 12.5 au,<sup>7</sup> which is the energy-minimized internuclear distance in the  $A^2\Sigma_u^+$  excited state.<sup>17</sup> Figure 1c shows the representation for the internuclear distance of 2.00 au and the H:2p nuclear charge of 3.90e, which is equal to the effective nuclear charge for 2p in nitrogen.<sup>12</sup> In the plots shown in Figures 1b and 1c, the two centered lobes are clearly evident in addition to the two lobes at both of the ends, and thus Figures 1b and 1c are consistent with the figures adopted in the textbooks, that is, Figure 2. From these results, it is thought that the radial distribution of the H:2p AO function given in the textbook and used in Figure 1a is too large for  $H_2^+$  whose internuclear distance is 2.00 au and the nuclear charge is  $e$ . This is the reason why Figure 1a is different in MO shape from Figure 2.

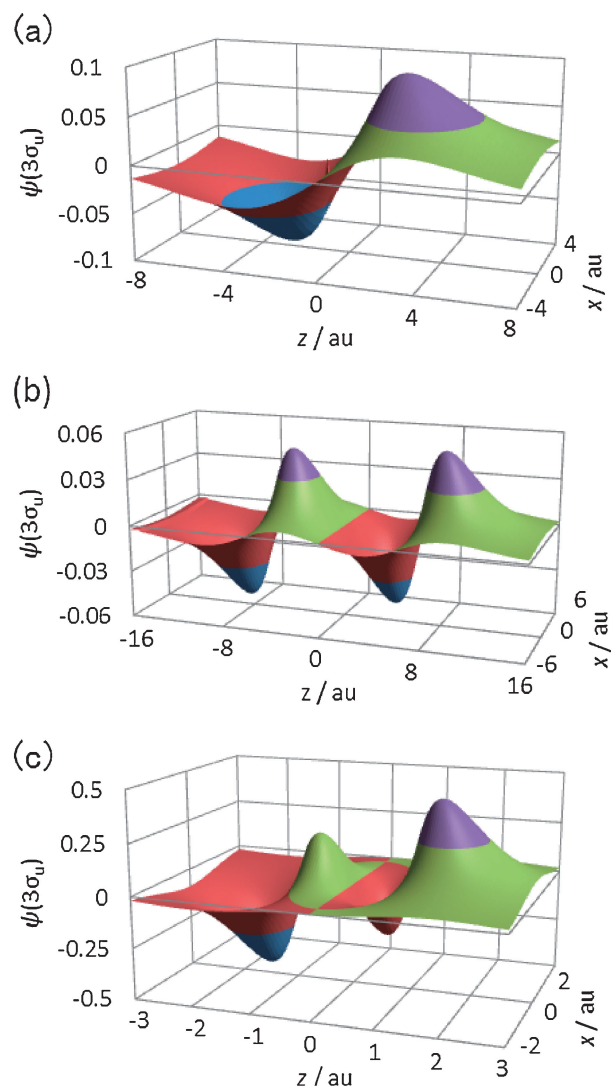


**Figure 1.** 3D contour representation of amplitude of  $H_2^+:3\sigma_u$  antibonding orbital in a plane containing two H nuclei. The MOs plotted in this figure were obtained by linear combination of two H:2p AOs (see the text). (a) The internuclear distance is 2.00 au.<sup>3</sup> (b) The internuclear distance is 12.5 au. (c) The internuclear distance and the nuclear charge are 2.00 au and 3.90e, respectively.

### ◆ Lithium Hydride (LiH)

Lithium hydride LiH is the simplest *neutral* heteronuclear diatomic molecule, and the bonding is often regarded as an example of ionic bonding.<sup>16b,19b,20</sup> Although hydrogen fluoride HF has a typical ionic bond (see the next section), the number of electrons contained in LiH (4) is much less than in HF (10). Accordingly, LiH gives a much simpler MO picture in ionic bonding than HF, and the simpler picture is very useful for explanation in quantum chemistry.

MOs of LiH can be described according to AOs of the Li and H atoms obtained on dissociation (separated atom description<sup>1a</sup>). Here, neutral Li and H instead of  $Li^+$  and  $H^-$  are used as the separated species, because in the gas phase the neutral separated ground-state atoms  $Li + H$  are more stable than the ground-state separated ions  $Li^+ + H^-$ .<sup>1c</sup> This stability difference

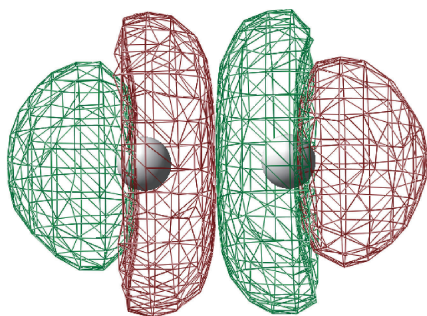


**Figure 2.** Real representation of  $\text{H}_2^+ : 3\sigma_u$  antibonding orbital calculated by using the ab initio MO method. The internuclear distance used in the calculation was 2.00 au. The red and green wireframes show positive- and negative-valued lobes of the orbital, respectively. Representations similar to this figure are adopted in various textbooks of quantum chemistry.<sup>1d,19a</sup>

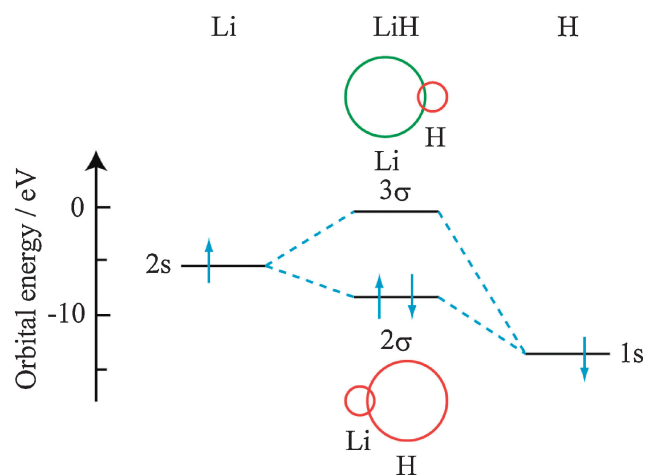


**Figure 3.** Computational energy-level diagram of Li:2s, H:1s, LiH:2σ, and LiH:3σ orbitals. The red and green circles respectively stand for the AOs with positive and negative values at their outer regions, and the radius denotes the magnitude of the AO coefficient in the MO. Basically, Li:1s AO does not participate in chemical bonding.

between  $\text{Li} + \text{H}$  and  $\text{Li}^+ + \text{H}^-$  was confirmed by our calculations using the ab initio MO method. If the nuclei are slowly pulled apart, a gas-phase LiH molecule will dissociate to the neutral atoms ( $\text{Li} + \text{H}$ ). Accordingly, to form 2σ bonding and 3σ antibonding orbitals of lithium hydride (LiH:2σ and 3σ, respectively), 2s AO of lithium (Li:2s) combines with 1s AO of hydrogen (H:1s), which is substantially lower in energy than Li:2s. H:1s makes a larger contribution to LiH:2σ. The opposite is true for LiH:3σ, in which the dominant component comes from Li:2s. Two LiH:2σ electrons are not equally shared between the Li and H atoms but are nearly localized at the H atom. The localization brings about an ionic character ( $\text{Li}^+ - \text{H}^-$ ) in the Li–H bond.

Figure 3 shows the computational energy-level diagram of the Li:2s, H:1s, LiH:2σ, and LiH:3σ orbitals. The orbital energies in the figure were estimated with our ab initio MO calculations.<sup>11</sup> The computational energies of the Li:2s, H:1s, and LiH:2σ orbitals shown in Figure 3 are consistent with the

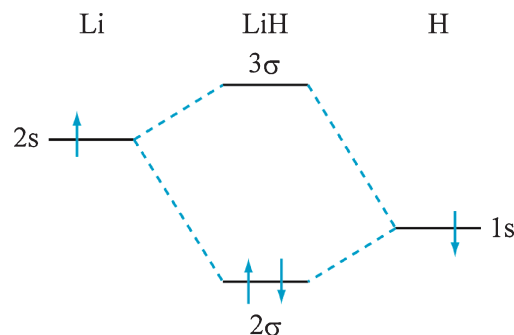


**Figure 4.** MO energy-level diagram of LiH adopted in some quantum chemistry textbooks.<sup>16b,19b,20</sup>

ionization energies experimentally obtained<sup>21</sup> when Koopmans' theorem<sup>1f</sup> is assumed to be valid. In Figure 3, the LiH:2σ bonding-orbital energy level lies between the Li:2s and H:1s AO levels, and LiH:2σ is higher in energy than H:1s by about 5 eV.<sup>22</sup> This computational energy-level diagram is not consistent with the diagrams adopted in some quantum chemistry textbooks.<sup>16b,19b,20</sup> In the textbooks, the energy-level diagram is schematically drawn like Figure 4, in which the LiH:2σ bonding orbital is lower in energy than each of the H:1s and Li:2s AOs. The LiH:2σ MO in our computational results (Figure 3) is less stabilized than in the conventional diagram (Figure 4).

The inconsistency between Figures 3 and 4 comes from the fact that the repulsion energy between the two LiH:2σ electrons is neglected in Figure 4 although the two electrons are nearly localized at the H atom. In contrast, the electron–electron repulsion is fully included by nature in our ab initio computational results shown in Figure 3. Since the electron–electron repulsion due to the electron localization at the H atom raises the LiH:2σ energy level, the LiH:2σ MO in Figure 3 lies at higher energy than in Figure 4. However, in  $\text{LiH}^+$  where such repulsion is absent, the calculated  $\text{LiH}^+ : 2\sigma$  MO energy (−20.24 eV) is lower than the H:1s energy (−13.60 eV).

In the MO energy-level diagram adopted in conventional quantum chemistry texts, only the electron–nuclear attraction energy and the nuclear–nuclear repulsion energy are taken into account,<sup>23</sup> and the electron–electron repulsion energy is neglected. Such a view is reasonable when two electrons in a bonding orbital are equally shared between two atoms. The shared electrons in the bonding orbital then interact with the two nuclei instead of one, and the sharing lowers the average electronic potential energy. The stabilization energy due to the electron sharing is generally greater than the electron–electron repulsion energy, and the neglect of the repulsion does not have a large influence on the MO energy-level diagram (Figure 5a). However, when the two electrons are nearly localized and the spatial overlap between them is large as in ionic bonds, the MO energy-level diagram needs a correction for the electron–electron repulsion energy (Figure 5b). Thus, the usual explanations for the Li–H bonding given in the textbooks are apt to be misleading.

Next we will roughly estimate the repulsion energy between the two LiH:2σ electrons localized at the H atom.<sup>11</sup> In the estimation, we assume that the repulsion energy in the LiH:2σ MO is much greater than the above-mentioned stabilization energy due to the electron sharing. The 1s AO energy of  $\text{H}^-$  ion

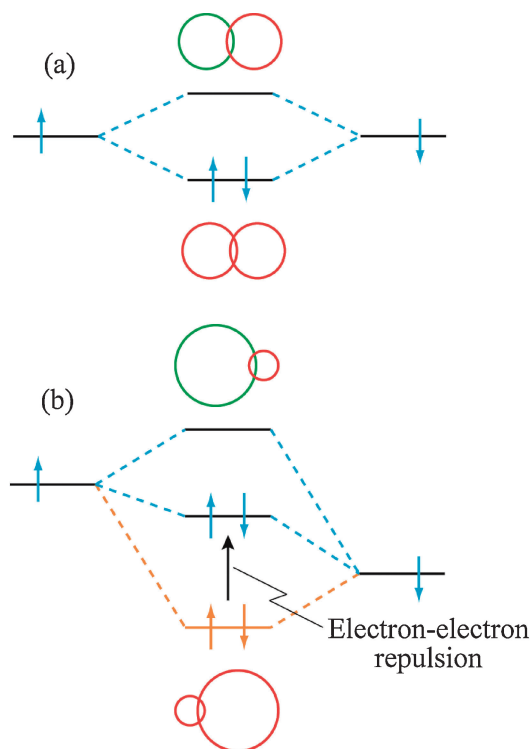


**Figure 5.** Schematic MO energy-level diagram. The red and green circles respectively stand for the AOs with positive and negative values at their outermost regions, and the radius denotes the magnitude of the AO coefficient in the MO. (a) Two electrons in a bonding orbital are equally shared between two atoms (for example, MOs of  $H_2$ ). The electron–electron repulsion energy is negligible. (b) Two electrons in a bonding orbital are localized, and the spatial overlap between them is large (for example, MOs of  $LiH$ ). The electron–electron repulsion raises the bonding-orbital energy level.

was calculated to be  $-1.16$  eV, which is higher than that of  $H:1s$  ( $-13.60$  eV) by  $12.44$  eV owing to the repulsion between the two localized  $1s$  electrons in  $H^-$ . Accordingly, when one full electron is transferred to a H atom in MO formation through combination of two AOs and when two electrons in the MO are localized at the H atom, the MO energy level is expected to rise by  $12.44$  eV from the original  $H:1s$  AO level. On the other hand, the Mulliken atomic charge<sup>18</sup> at the H atom of  $LiH$  was estimated to be  $-0.414$ , which shows that in the  $LiH:2\sigma$  MO formation,  $41.4\%$  of the  $Li:2s$  electron is transferred to the H atom without any transfer of the  $H:1s$  electron to the Li atom. The spatial overlap between this  $Li \rightarrow H$  transferred electron and the original  $H:1s$  electron raises the  $LiH:2\sigma$  orbital energy level. Since  $12.44$  eV multiplied by  $0.414$  is  $5.15$  eV, the  $LiH:2\sigma$  energy level is expected to rise by about  $5$  eV from the original  $H:1s$  level. The energy rise thus estimated is consistent with Figure 3, where  $LiH:2\sigma$  is higher in energy than  $H:1s$  by about  $5$  eV.

### ◆ Hydrogen Fluoride (HF)

The bonding of hydrogen fluoride (HF) is generally regarded as typical ionic bonding, and a MO energy-level diagram similar to Figure 4 is adopted for HF in conventional

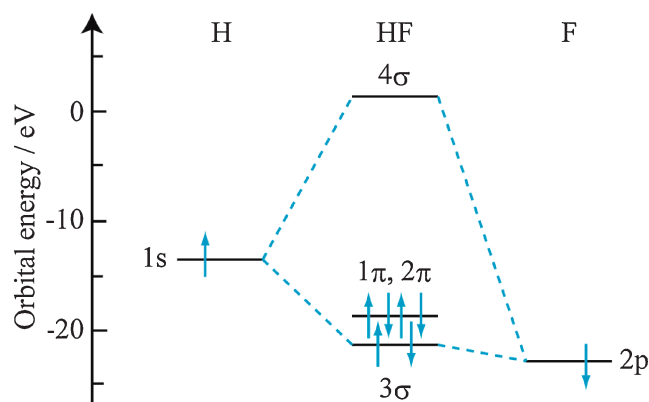


**Figure 6.** Computational energy-level diagram of  $H:1s$ ,  $F:2p$ ,  $HF:3\sigma$ ,  $HF:1\pi,2\pi$ , and  $HF:4\sigma$  orbitals. Here, the contribution from  $F:2s$  AO is not drawn, and the  $F:2p$  AO shown in the figure denotes the singly occupied AO. Basically,  $F:1s$  AO does not participate in chemical bonding. Note that in the gas phase the neutral separated ground-state atoms  $H + F$  are more stable than the ground-state separated ions  $H^+ + F^-$ ,<sup>1c</sup> similarly to the case of  $LiH$ . This stability difference between  $H + F$  and  $H^+ + F^-$  was confirmed by our ab initio MO calculations. If the nuclei are slowly pulled apart, a gas-phase HF molecule will dissociate to neutral atoms ( $H + F$ ).

textbooks of chemistry.<sup>9a,16b,24</sup> However, inconsistency similar to that between Figures 3 and 4 in  $LiH$  was found also in  $HF$ .<sup>11</sup> Figure 6 shows the computational energy-level diagram of  $H:1s$ ,  $F:2p$ ,  $HF:3\sigma$ ,<sup>25</sup>  $HF:1\pi,2\pi$ , and  $HF:4\sigma$  orbitals. The computational energies of the  $H:1s$ ,  $F:2p$ ,  $HF:3\sigma$ , and  $HF:1\pi,2\pi$  orbitals shown in Figure 6 are consistent with the photoelectron spectra experimentally obtained<sup>21</sup> when Koopmans' theorem<sup>1f</sup> is assumed to be valid. The  $HF:3\sigma$  bonding-orbital energy level lies between the  $H:1s$  and  $F:2p$  AO levels, and  $HF:3\sigma$  is higher in energy than  $F:2p$  by about  $2$  eV. The electron–electron repulsion due to the electron localization at the F atom again raises the  $HF:3\sigma$  energy level, which lies at higher energy in Figure 6 than in the MO energy-level diagram adopted in the textbooks. Thus, the usual explanations for the H–F bonding given in the textbooks are liable to misunderstanding. The situation shown in Figure 5b is generally seen in ionic bonding except that of  $HeH^+$  (the simplest heteronuclear diatomic molecule<sup>20</sup>), which will dissociate to He and  $H^+$  if the nuclei are slowly pulled apart.<sup>26</sup>

### ◆ Hybridization

Hybridization of AO is very useful in explanation of shapes and properties of organic molecules.<sup>10</sup> To form a hybrid orbital in carbon,  $C:2s$  and some  $C:2p$  AOs linearly combine with one another. As described in a previous section, the AO is given as the product of a radial function and a spherical harmonics function in a simple quantum-chemical picture. The 3D contour representation of *one* hybrid orbital in carbon thus constructed is consistent with the figures adopted in various textbooks of chemistry.<sup>3</sup>

On the other hand, Figure 7a shows the 3D contour representation of *three*  $sp^2$  hybrid orbitals in carbon included in a molecule such as  $CH_3^+$ , and its electron-density distribution



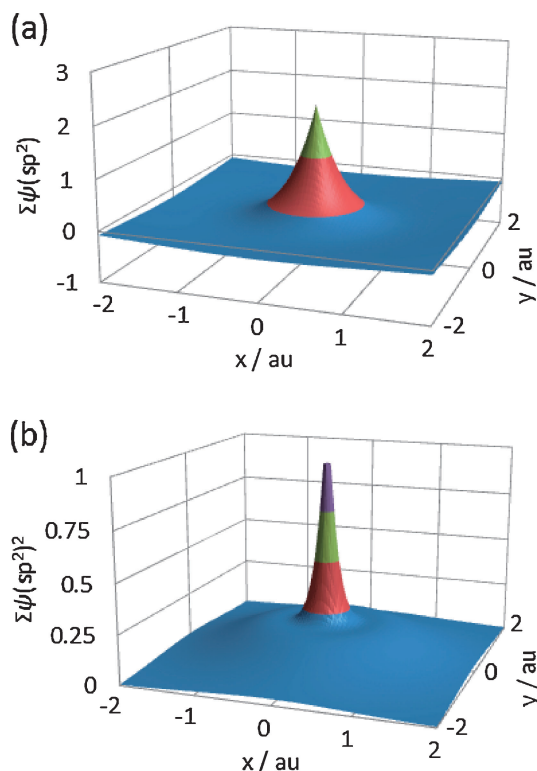


**Figure 7.** 3D-contour representation of three  $sp^2$  hybrid orbitals in carbon. The amplitude in the molecular plane is depicted. (a) Total orbital shape. (b) Electron-density distribution.

is depicted in Figure 7b.<sup>3</sup> These representations show the amplitudes ( $\Sigma\psi/sp^2$ ) and  $\Sigma\psi/(sp^2)^2$ ) in the molecular plane. Note that Figure 7a shows the total  $sp^2$ -orbital shape. The contour plots have circular symmetry, because the 3D orbital shape of the two C:2p AOs participating in the  $sp^2$  hybridization gives a doughnut-shaped surface (Figure 6.13 of Reference 1). As predicted by Tokita,<sup>27</sup> each of the contour plots shown in Figure 7 is not consistent with the schematic figures adopted for the  $sp^2$  hybrid orbitals in textbooks. The figures adopted in the textbooks<sup>10,16c</sup> are similar to a three-leaf clover (Figure 8b) and are entirely different from the contour representations shown in Figure 7. Accordingly, the schematic figures in the textbooks do not give the real total  $sp^2$ -orbital shape and do not show its real electron-density distribution, either. However, if one draws the three  $sp^2$  hybrid orbitals one by one on three different transparent sheets respectively and watches the orbitals through the three transparent sheets laid one on top of another (Figure 8), the three  $sp^2$  hybrid orbitals thus represented are close to the schematic figures adopted in the textbooks.

Similarly, the total  $sp^3$ -orbital shape and its electron-density distribution corresponding to the representations for  $sp^2$  shown in Figure 7 are not tetrahedral but have spherical symmetry,<sup>3</sup> in contrast to the schematic figures given in the textbooks.<sup>10,16c</sup> Furthermore, the total  $sp$ -orbital shape does not look like a dumbbell but has circular symmetry though its electron-density distribution is dumbbell-shaped.<sup>3</sup> Thus, the usual explanations for the hybrid orbitals given in the textbooks are apt to misleading.

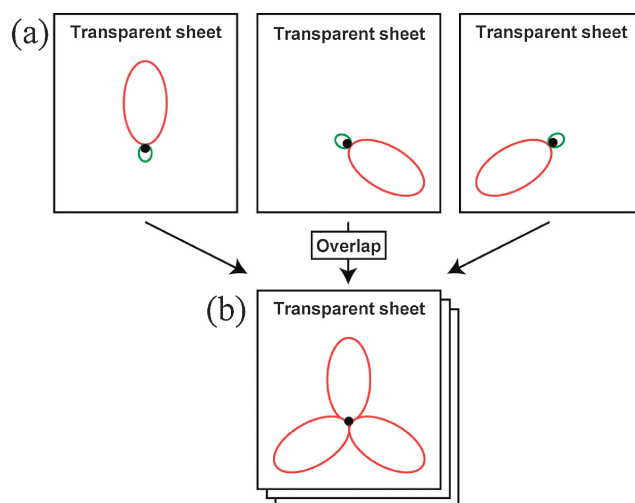


**Figure 8.** (a) Three  $sp^2$  hybrid orbitals drawn one by one on three different transparent sheets, respectively. (b) The three  $sp^2$  hybrid orbitals seen through the three transparent sheets laid one on top of another. Representations similar to Figure 8b are adopted in various textbooks of quantum chemistry.<sup>10,16c</sup>

### ◆ Summary and Future Perspectives

To revisit the MOs in  $H_2^+$ , LiH, HF, and hybridization, we have drawn the 3D contour plots of the  $H_2^+$  MOs and carbon hybrid orbitals according to the explanations given in textbooks of quantum chemistry and have also performed the ab initio MO calculations of LiH and HF. Some 3D contour representations and MO energy-level diagrams thus obtained are not consistent with the figures adopted in the textbooks. It is considered that the usual explanations for the MOs of  $H_2^+$ , LiH, HF, and hybridization in the conventional textbooks are liable to misunderstanding. We have revisited these simple subjects and have acquired useful ideas for better understanding of the MO method. We should stop believing various textbook explanations excessively and should examine them in detail once more. In this sense, the highest occupied MOs (HOMOs) in nitrogen ( $N_2$ ) and the related molecules need to be revisited.<sup>28</sup> Such a revisit would further shed new light on understanding of quantum chemistry.

We greatly acknowledge Dr. Takuhiro Kakiuchi and the practice trainees of Ehime University for their valuable suggestion. U.N. thanks Professor Emeritus Sumio Tokita of Saitama University who let him know Reference 27.

### References and Notes

- 1 a) I. N. Levin, *Quantum Chemistry*, 6th ed., Pearson, Upper Saddle River NJ, **2009**, Sect. 13.5. b) Sect. 6.1. c) Sect. 13.7. d) Sect. 13.6. e) Sect. 13.16. f) Sect. 11.1. g) Sect. 15.6. h) Sect. 14.3.
- 2 S. Nagaoka, *Chem. Educ.* **1992**, *40*, 600.
- 3 S. Nagaoka, H. Teramae, U. Nagashima, *J. Comput. Chem., Jpn.* **2010**, *9*, 177.
- 4 S. Nagaoka, H. Teramae, U. Nagashima, *J. Comput. Chem., Jpn.* **2010**, *9*, 241.
- 5 C. M. Quinn, *Computational Quantum Chemistry: An*

- Interactive Guide to Basis Set Theory*, Academic Press, London, **2002**, Sect. 1.1.
- 6 V. Walters, J. de Paula, P. Atkins, *Explorations in Physical Chemistry*, 2nd ed., Oxford University Press, Oxford, **2007**.
  - 7 A. V. Turbiner, H. Olivares-Pilón, *J. Phys. B: At., Mol. Opt. Phys.* **2011**, *44*, 101002.
  - 8 F. Holka, P. G. Szalay, J. Fremont, M. Rey, K. A. Peterson, V. G. Tyuterev, *J. Chem. Phys.* **2011**, *134*, 094306.
  - 9 a) P. Atkins, T. Overtone, J. Rourke, M. Weller, F. Armstrong, *Shriver & Atkins' Inorganic Chemistry*, 5th ed., Oxford University Press, Oxford, **2010**, Chap. 2. b) Chap. 4.
  - 10 K. P. C. Vollhardt, N. E. Schore, *Organic Chemistry: Structure and Function*, 6th ed., Freeman, New York, **2011**, Sect. 1.8.
  - 11 A. Sagan, U. Nagashima, H. Teramae, S. Nagaoka, *J. Comput. Chem., Jpn.* **2011**, *10*, 75.
  - 12 J. A. Pople, D. L. Beveridge, *Approximate Molecular Orbital Theory*, McGraw-Hill, New York, **1970**, Sect. 1.9.
  - 13 A. D. McLean, G. S. Chandler, *J. Chem. Phys.* **1980**, *72*, 5639.
  - 14 R. Krishnan, J. S. Binkley, R. Seeger, J. A. Pople, *J. Chem. Phys.* **1980**, *72*, 650.
  - 15 M. J. Frisch, G. W. Trucks, H. B. Schlegel, G. E. Scuseria, M. A. Robb, J. R. Cheeseman, J. A. Montgomery, Jr., T. Vreven, K. N. Kudin, J. C. Burant, J. M. Millam, S. S. Iyengar, J. Tomasi, V. Barone, B. Mennucci, M. Cossi, G. Scalmani, N. Rega, G. A. Petersson, H. Nakatsuji, M. Hada, M. Ehara, K. Toyota, R. Fukuda, J. Hasegawa, M. Ishida, T. Nakajima, Y. Honda, O. Kitao, H. Nakai, M. Klene, X. Li, J. E. Knox, H. P. Hratchian, J. B. Cross, V. Bakken, C. Adamo, J. Jaramillo, R. Gomperts, R. E. Stratmann, O. Yazyev, A. J. Austin, R. Cammi, C. Pomelli, J. W. Ochterski, P. Y. Ayala, K. Morokuma, G. A. Voth, P. Salvador, J. J. Dannenberg, V. G. Zakrzewski, S. Dapprich, A. D. Daniels, M. C. Strain, O. Farkas, D. K. Malick, A. D. Rabuck, K. Raghavachari, J. B. Foresman, J. V. Ortiz, Q. Cui, A. G. Baboul, S. Clifford, J. Cioslowski, B. B. Stefanov, G. Liu, A. Liashenko, P. Piskorz, I. Komaromi, R. L. Martin, D. J. Fox, T. Keith, M. A. Al-Laham, C. Y. Peng, A. Nanayakkara, M. Challacombe, P. M. W. Gill, B. Johnson, W. Chen, M. W. Wong, C. Gonzalez, J. A. Pople, *Gaussian 03 (Revision C02)*, Gaussian, Inc., Wallingford CT, **2004**.
  - 16 a) C. Fukuma, *Quantum Chemistry Notes*, Kodansha, Tokyo, **2004**, Chap. 7. b) Chap. 12. c) Chap. 13.
  - 17 G. Herzberg, *Molecular Spectra and Molecular Structure I: Spectra of Diatomic Molecules*, Van Nostrand Reinhold, New York, **1950**, Sect. VI.4.
  - 18 L. J. Schaad, W. V. Hicks, *J. Chem. Phys.* **1970**, *53*, 851.
  - 19 a) G. C. Pimentel, R. D. Spratley, *Chemical Bonding Clarified through Quantum Mechanics*, Holden-Day, San Francisco, **1969**, Sect. 4.2. b) Sect. 3.5b.
  - 20 W. J. Moore, *Physical Chemistry*, 4th ed., Prentice-Hall, Englewood Cliffs NJ, **1972**, Sect. 15.13.
  - 21 <http://webbook.nist.gov/chemistry/> (accessed December 2011).
  - 22 Li-H bond is a stable ionic bond though twice of the LiH:2 $\sigma$  bonding-orbital energy ( $-16.37$  eV) is higher than the sum of the Li:2s and H:1s AO energies ( $-18.94$  eV) (Figure 3). Note that the Hartree-Fock energy is not determined by the orbital energies alone.<sup>1h</sup>
  - 23 Strictly speaking, two other effects may also contribute to the bonding formation.<sup>1a</sup>
  - 24 P. Atkins, J. de Paula, *Physical Chemistry*, 9th ed., Oxford University Press, Oxford, **2010**, Sect. 10.5.
  - 25 1 $\sigma$ , 2 $\sigma$ , and 3 $\sigma$  in the MO energy-level diagram of HF adopted in Reference 9a should read 2 $\sigma$ , 3 $\sigma$ , and 4 $\sigma$ , respectively.
  - 26 A. Sagan, S. Nagaoka, H. Teramae, U. Nagashima, *J. Comput. Chem., Jpn.*, in press.
  - 27 S. Tokita, *MaLS Forum* **2006**, *4*, 2; This reference is available electronically on the Web site, <http://sucra.saitama-u.ac.jp/modules/xoonips/detail.php?id=KY-AA11910807-45> (accessed December 2011).
  - 28 A. Sagan, S. Nagaoka, H. Teramae, U. Nagashima, *J. Comput. Chem., Jpn.*, submitted.